

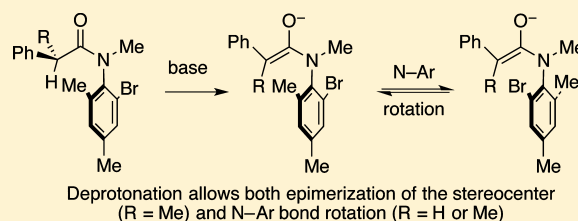
Rotational Isomers of *N*-Methyl-*N*-arylacetamides and Their Derived Enolates: Implications for Asymmetric Hartwig Oxindole Cyclizations

J r mie Mandel, Xiaohong Pan, E. Ben Hay, Steven J. Geib, Craig S. Wilcox,* and Dennis P. Curran*

Department of Chemistry, University of Pittsburgh, Pittsburgh, Pennsylvania 15260, United States

S Supporting Information

ABSTRACT: The rotational preferences of *N*-(2-bromo-4,6-dimethylphenyl)-*N*-methyl-2-phenylpropanamide were studied as a model of precursors for Hartwig asymmetric oxindole cyclizations. The atropisomers of this compound were separated by flash chromatography, and then the enantiomers were resolved and the interconversions of the stereocenter and the *N*–*Ar* axis were studied. Under thermal conditions, the axis is very stable. Under the basic conditions of the Hartwig cyclization, both the stereocenter and the chiral axis equilibrate via enolate formation. The *N*–*Ar* rotation barrier of a 2-phenylacetamide analogue was reduced from 31 kcal mol^{−1} in the precursor to 17 kcal mol^{−1} in the enolate. Reasons for this dramatic barrier reduction and implications of both *N*–*Ar* and amide C–*N* rotations for Hartwig cyclizations are discussed.



INTRODUCTION

Rotational isomerism of *N*sp²–*C*sp² single bonds spans the full range of possibilities depending on substituents. At one end, amide and related functional groups are planar and exhibit *E/Z* isomerism.¹ At the other end, functional groups with *N*sp²–*Ar* and related cores often prefer twisted, even orthogonal, geometries. Such groups include *N*-arylamides, carbamates, ureas, heterocycles (lactams, imides, among many others), and so on.^{2,3} Both the geometry of the *N*–*Ar* bond and its rotation barrier are crucial features in areas as diverse as enzyme/substrate binding,⁴ molecular torsional balances,⁵ and asymmetric synthesis.⁶

When reactive intermediates are involved, asymmetric reactions of axially chiral anilides (*N*-arylamides) are often ultimately dictated by the configuration of the starting material.^{6,7} This is because the onward reactions of the intermediates, radicals, anions,^{6,8} and organometallic species,⁸ are faster than one or more bond rotations. The result is that only a subset of the usually considered transition states is actually available for onward reaction in one atropisomer of a starting material. The remaining subset is only accessible from the other atropisomer.

Consider asymmetric Heck reactions of the *o*-iodoanilides, as shown in Figure 1a. These were pioneered by Overman for use in natural product synthesis.¹⁰ Cyclization of *o*-haloanilides like **1** with various chiral palladium catalysts produces 3-alkenyl-2-oxindoles **2** in high yields and ee's. Like most anilides, precursors **1** prefer the (*E*)-amide rotamer (*N*–*Ar* and C=O are trans), and the plane of the *N*–*Ar* group is roughly orthogonal to the plane of the amide.¹¹

To address the question of which step in the Heck reaction dictates the enantioselectivity, we prepared enantioenriched **3** that has an added *o*-methyl group (shown in red) to "lock" the *N*–*Ar* bond. Then we conducted Heck cyclizations with an

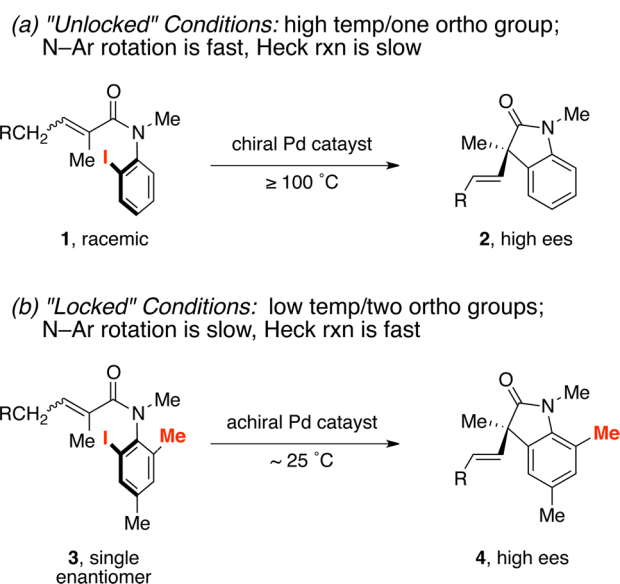


Figure 1. Asymmetric Heck reactions of anilide atropisomers. Two limiting conditions: *N*–*Ar* axis unlocked (a) or locked (b).

achiral palladium catalyst under ambient temperature conditions where the lock was in effect (Figure 1b).⁹ High chirality transfer from the axis of **3** to the stereocenter of **4** was observed. This shows that *N*–*Ar* bond rotation does not occur during the Heck process of the locked substrate **3**. It also suggests that asymmetric Heck reactions like those in Figure 1a under "unlocked" conditions might be dynamic kinetic resolutions where the stereochemistry-determining step is

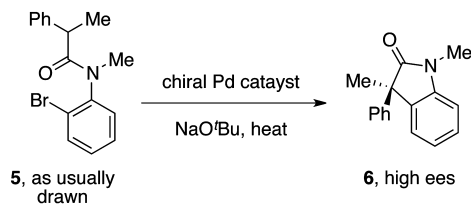
Received: February 25, 2013

Published: March 28, 2013

oxidative addition of a chiral Pd species into one of the rapidly equilibrating atropisomers of **1**.

A second class of asymmetric reactions of *o*-haloanilides, Pd-catalyzed enolate cyclizations, also produce oxindoles (Figure 2a). These transformations were pioneered by Lee and

(a) Hartwig asymmetric oxindole cyclizations



(b) Precursor **5** has three stereogenic elements

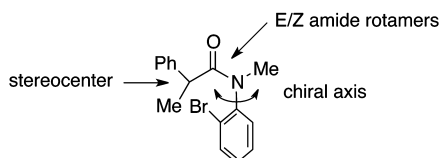


Figure 2. Hartwig cyclizations of *o*-haloanilide enolates provide enantioenriched oxindoles (a) and stereogenic elements of their precursors (b).

Hartwig,¹² and several groups have introduced new chiral ligands.¹³ Kündig's NHC ligands, in particular, give exceptional ees with broad substrate scope.^{13b} Generally speaking, cyclization of *o*-haloanilides like **5** with a strong base (to make the enolate) and a chiral catalyst provides 3-phenyl-2-oxindoles **6**.¹⁴ The mechanism of this reaction may be very different from a Heck reaction, and Hartwig provided evidence for palladacycle intermediates.^{12,13e}

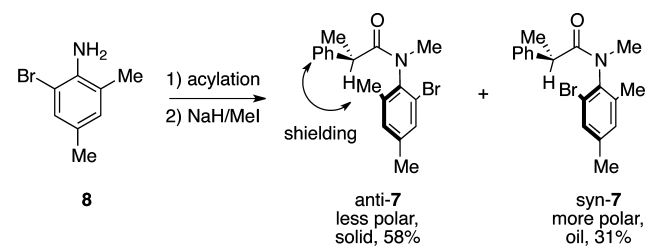
We set out to answer two questions about this reaction. First, the commonly drawn depictions of **5** with a planar (*Z*)-amide cannot represent energy minima. Precursors like **5** have three stereogenic elements, the stereocenter, the amide C–N bond, and the N–Ar axis (Figure 2b). What do molecules like **5** look like in the ground state? And second, does the configuration of either the stereocenter¹⁵ or the chiral axis play a key role in these cyclizations?

To address both questions, we made and studied cyclizations of stereoisomerically pure “locked” precursors bearing additional *o*-methyl groups. Here we show that such precursors exist mostly as two diastereomers, both of which have an (*E*)-amide bond. To our surprise, the lock was cracked under Hartwig cyclization conditions, apparently because the amide enolate has a much lower N–Ar rotation barrier than its conjugate acid precursor. We report N–Ar rotation barriers for two substrates in both protonated and enolate forms, and we discuss the consequences of this reaction on Hartwig oxindole cyclizations.

RESULTS AND DISCUSSION

We selected *N*-methyl-*N*-(2-bromo-4,6-dimethylphenyl)-2-phenylpropanamide **7** as the “locked” precursor for resolution and cyclization (Scheme 1). The added *o*-methyl group serves as the lock by raising the N–Ar rotation barrier; however, this methyl group is not expected to significantly alter either ground-state geometry or isomer populations relative to **5**.^{7a,b,9,11} The added *p*-methyl group in **7** should not significantly affect either barriers or rotamer populations, and

Scheme 1. Synthesis and Separation of the Racemic Syn/Anti Atropisomers of **7** Shown in *R* Enantiomeric Series



it is present simply because the precursor (2-bromo-4,6-dimethylaniline, **8**) is readily available.

Acylation of **8** with *rac*-2-phenylpropanoyl chloride followed by alkylation of the resulting *sec*-amide with NaH and iodomethane provided a mixture of *N*-methylated atropisomers **7**. These were readily separated by flash chromatography. The less polar isomer *anti*-**7** was isolated in 58% yield as a white solid, while the more polar isomer *syn*-**7** was isolated as a clear oil in 31% yield. Here “*syn*” and “*anti*” refer to the orientations of the bromine atom on the aryl ring relative to the phenyl group on the stereocenter in the depicted conformation. The combined yield of the two racemates was 89%.

Relative configurations of **7** were assigned by NMR spectroscopy with the assumption that geometries like that shown in Scheme 1 are favored. Specifically, the C–H bond of the stereocenter is oriented approximately anti to the amide carbonyl group. The major isomer *anti*-**7** has a shielded singlet at 1.41 ppm in its ¹H NMR spectrum. We assign this to the *o*-methyl group and attribute the upfield shift to anisotropic shielding by the phenyl ring. The *p*-methyl group in *anti*-**7** and both aryl methyl groups of *syn*-**7** resonate in a narrow range 2.31–2.34 ppm.

Both diastereomers were resolved into their enantiomeric components by preparative chiral HPLC on an (*S,S*)-Whelk-O1 column, with the *anti* diastereomer providing *S,M*-**7** and *R,P*-**7** and the *syn* diastereomer providing *S,P*-**7** and *R,M*-**7**. The absolute configuration of enantiomer *R,P*-**7** was determined by solving its X-ray crystal structure (Figure 3), which also confirmed the *anti* relative configuration of both the N–Ar axis and *E*-geometry of the amide C–N bond.

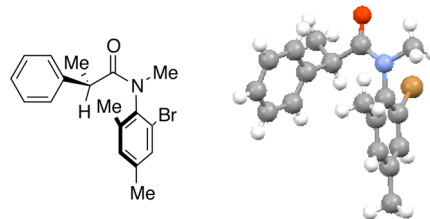


Figure 3. Ball and stick representation of the X-ray crystal structure of *anti*-isomer *R,P*-**7**.

The last link in the structure assignment, absolute configurations of the *syn* diastereomers of **7**, was provided by heating the *anti* diastereomers to induce N–Ar bond rotation; *R,P*-**7** equilibrated with *R,M*-**7** and *S,P*-**7** with *S,M*-**7**. A complete rotation profile in the (*R*)-enantiomeric series is shown in Figure 4. The N–Ar atropisomers (*anti*/*syn*) do not interconvert at rt, but each (*E*)-amide rotamer is in equilibrium with the corresponding (*Z*)-amide rotamer (N–Ar and C=O *cis*), which must also be twisted into two atropisomers, as

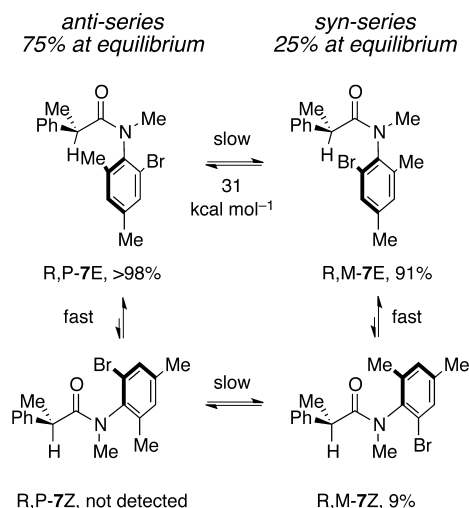


Figure 4. Interconversion of rotational isomers of **7** shown in the *R* enantiomeric series. At rt, amide *E/Z* rotation (vertical) is fast but *N*–*Ar* rotation (horizontal) is very slow.

shown. In CDCl_3 at rt, the minor amide rotamer *R,P*-**7Z** in the anti series cannot be identified in the ^1H NMR spectrum of the major atropisomer (*R,P*-**7E**/*R,P*-**7Z** > 98/2), while the *E/Z* ratio in the minor syn-atropisomer series, *R,M*-**7E**/*R,M*-**7Z**, is about 91/9.

The interconversion of antiatropisomer *R,P*-**7** and syn-atropisomer *R,M*-**7** was studied by heating pure samples of each isomer at 100°C in *tert*-butylbenzene with time course monitoring by ^1H NMR spectroscopy. The equilibrium ratio is about 75/25 in favor of *R,P*-**7**. Data were processed in the usual way (see the Supporting Information) to give a barrier from *M* to *P* (minor to major) of $\Delta G^\ddagger = 30.5 \text{ kcal mol}^{-1}$, while the barrier from *P* to *M* (major to minor) is $\Delta G^\ddagger = 31.2 \text{ kcal mol}^{-1}$. These barriers mean that the atropisomers of **7** have significant stability under the thermal conditions of Hartwig reactions ($t_{1/2}$ of several days at 85°C compared to reactions times of several hours).

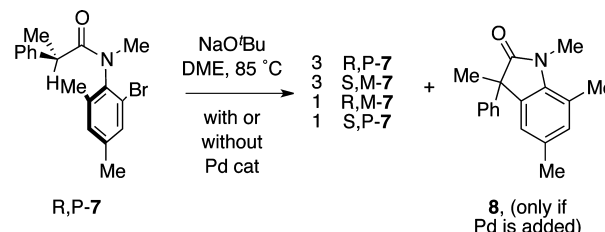
Neglecting temperature dependence of equilibrium constants, *R*-**7** exists at equilibrium as about 75% of antiseries isomer *R,P*-**7E**, 23% of syn-series isomer *R,M*-**7E** and 2% of its amide rotamer *R,M*-**7Z**. The fourth isomer *R,P*-**7Z** (amide rotamer of the major isomer) is present only in trace amounts.

The depiction in Figure 4 implies that the mechanism for *N*–*Ar* bond rotation is direct interconversion of *R,P*-**7E** and *R,M*-**7E**. This is not necessarily the case because equilibration could occur over the *Z*-isomers in a Curtin–Hammett scheme or could even be geared (coupled) with amide rotation.¹⁸ Nonetheless, it is the magnitude of the barrier, not the mechanism of the process, that is important for the forthcoming discussion. Here we focus on the major (*E*)-amide rotamers (98% total), but these are in equilibrium with small amounts of the corresponding (*Z*)-rotamers (2% total).

We next conducted control experiments by exposing *R,P*-**7** to NaO^tBu in DME at 85°C . These are typical conditions for asymmetric Hartwig cyclizations,^{12,13} but we omitted the palladium and ligands. Reaction progress was followed by chiral HPLC. We expected to see one new isomer from base-catalyzed epimerization of the stereocenter, but we quickly saw all three of the other isomers and the system soon reached equilibrium (3/3/1/1). Thus, the base promotes isomerization of both the stereocenter and, unexpectedly, the *N*–*Ar* axis.

We conducted a few experiments with the stereopure precursors in the presence of palladium catalysts and NHC ligands with similar results.^{16,17} In other words, the precursors **7** approached full equilibrium at a rate that was faster than formation of product **8** (Scheme 2). This shows the

Scheme 2. Base-Catalyzed Equilibration of Both the Stereocenter and the Axis of **7** Occurs with or without a Pd Catalyst and Ligand



stereocontrol in the Hartwig reaction is not dictated by the original stereocenter,¹⁵ but it also shows that the “locked substrate” approach cannot be used to test for the importance of *N*–*Ar* atropisomer configuration in the Hartwig reaction because the base cracks the lock.

The results suggest that the mechanism for cracking the lock is simply formation of the enolate. Deprotonation of course equilibrates the stereocenter (by reversible protonation), but it also must allow for rotation of the *N*–*Ar* axis of rotamers *P*-**9** and *M*-**9**, as shown in Figure 5. Deprotonation can form

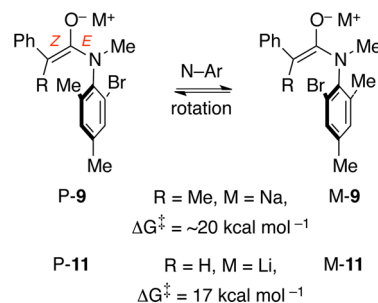


Figure 5. Enolate atropisomers based on *N*–*Ar* bond rotation and illustrated with *E*-amide–*Z*-enolates.

isomeric amide (*E/Z*)-enolates. But it erases the stereocenter, so in a simple view the diastereomers of **7** become enantiomers. The rotation is illustrated with (*Z*)-enolates (Ph and OM *cis*), but (*E*)-enolates or even twisted (chiral) enolates may also be present.

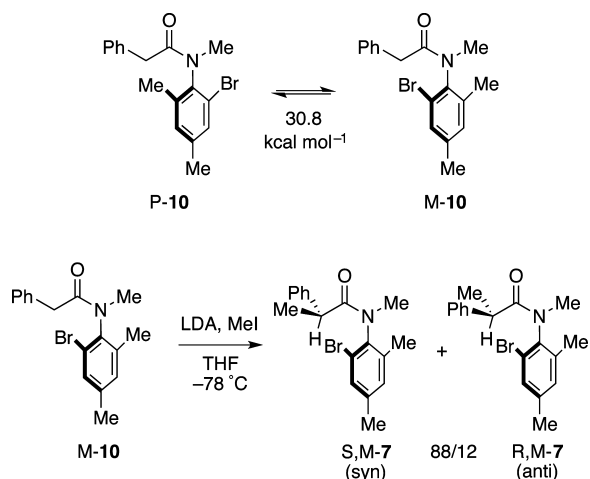
A time course experiment at 0°C allowed us to estimate that the barrier for *N*–*Ar* rotation is reduced from 31 kcal mol^{-1} in the precursor to about 20 kcal mol^{-1} in the enolate. This is a large effect, especially considering that the amide and the enolate both get their axial chirality from two adjacent sp^2 centers.

The measured value of *N*–*Ar* rotation of the enolate **9** is only a crude estimate for at least two reasons: (1) the kinetic analysis is inherently problematic because two interconversions (epimerization and *N*–*Ar* bond rotation) occur more or less simultaneously, and (2) the analysis assumes that the deprotonation is quantitative, which may not be the case.^{13f} To make a more clear-cut measurement of an enolate *N*–*Ar* rotation barrier, we removed the α -methyl group from **7** to

eliminate the stereocenter and we switched to a stronger base to ensure complete deprotonation.

rac-*N*-(2-Bromo-4,6-dimethylphenyl)-2-phenylacetamide **10** was synthesized and then preparatively resolved into its two enantiomers on an (*S,S*)-Whelk-O1 HPLC column (Scheme 3). Standard thermal equilibration experiments as above

Scheme 3. Interconversion of Stropisomers of **10 and Assignment of Absolute Configuration by Methylation of the Enolate**



provided the barrier to interconversion of the two atropisomers, $\Delta G^\ddagger = 30.8 \text{ kcal mol}^{-1}$. Scheme 3 shows only the major (*E*)-amide rotamer of **10**, but the (*Z*)-rotamer can be observed by ^1H NMR spectroscopy and the *E/Z* ratio at rt in CDCl_3 is about 96/4.

To assign the absolute configuration of the atropisomers, we deprotonated the first eluting enantiomer with lithium diisopropylamide (LDA) at -78°C and then added iodomethane at the same temperature. To ensure that no *N*–*Ar* bond rotation occurred, the reaction was quenched with NH_4Cl after 10 min, and then the products were assessed by chiral HPLC. About 60% of the mixture was methylated products *S,M*-7 and *R,M*-7 in a ratio of 88/12. The remaining 40% was recovered *M*-10. No *P*-atropisomers of either the precursor **10** or the products were detected by chiral HPLC, so *N*–*Ar* rotation of the lithium enolate is slow relative to methylation at -78°C . A similar experiment with *P*-**10** gave the atropisomers *S,P*-7 and *R,P*-7 with similar conversion and ratio.

The enolate methylation provides the less stable syn-atropisomer in excess, and the diastereoselectivity (88/12) is surprisingly high given that the two *ortho* substituents (Me and Br) shielding the two faces of enolate **11** are not that different in size. This selectivity is even more surprising in light of the results of Simpkins and co-workers.^{7h,i} They observed low selectivities with related axially chiral enolates that appear to be much more favorably biased for face selectivity (one *o*-substituent is H and the other is *t*Bu). They attributed the low selectivity to alkylation of *Z*-amide–*Z*-enolates in competition with *E*-amide–*Z*-enolates.

Compared to enolate **9**, the structure of enolate **11** derived from **10** and lacking the α -methyl group is more clear-cut (Figure 5). Amide enolates with only one substituent on the anionic carbon atom adopt a planar, (*Z*)-enolate geometry to avoid A-strain between the enolate substituent (here Ph) and one of the *N*-substituents (here the *Ar* ring).¹⁹ Thus, the

geometries of **11** in Figure 5 are probably good approximations of solution structures.

To measure the *N*–*Ar* rotation barrier of the enolate, **11** was added to a solution of LDA at -38°C , and then aliquots were periodically quenched and ee was assessed by chiral HPLC. Despite possible complexities with enolate aggregates, reasonable first-order kinetics were observed with $\Delta G^\ddagger = 17 \text{ kcal mol}^{-1}$. A similar experiment at -45°C gave a comparable result (see the Supporting Information). Thus formation of the enolate reduces the *N*–*Ar* rotation barrier by almost 14 kcal mol^{-1} .

The origin of the barrier decrease is cloaked in the structure of the enolate. Like its amide precursor, enolate **11** has both *N*–*Ar* and *N*–*C*(*O*)=*C* rotamers, the latter being the analogue of *E/Z* amide rotamers. Thus, *N*–*Ar* rotation could occur either on an (*E*) or a (*Z*) amide enolate rotamer or even be coupled to amide enolate rotation.

In resonance terms, deprotonation of an amide **10** introduces cross-conjugation in the resulting amide enolate **11** (Figure 6).

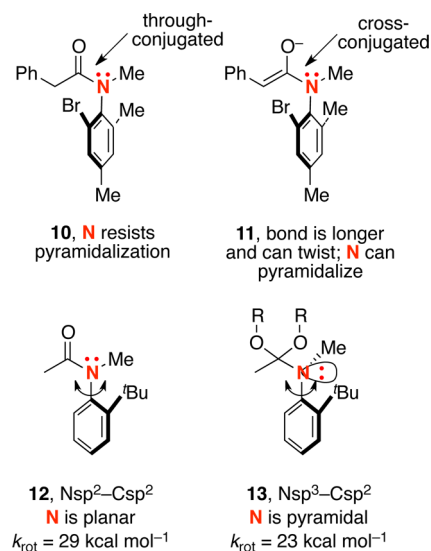


Figure 6. Suggested effects of pyramidalization: conversion of an anilide to an enolate or *o*-anilide allows pyramidalization at *N* and reduces the *N*–*Ar* rotation barrier.

This suggests that carbamates and ureas might be simple models for amide enolates. The cross-conjugation in carbamates and ureas lowers the *C*(*O*)–*N* bond rotation barrier (*E/Z* isomerization) relative to comparable amides.²⁰ In addition, the *N*–*Ar* rotation barriers of *N*-aryl carbamates and ureas are also lower than those of comparable *N*-aryl amides (anilides).²¹ Thus, the barrier-reducing effect of cross-conjugation still plays out at the *N*–*Ar* bond even though the two connected π -systems (carbamate/urea and aryl ring) are orthogonal. Presumably, cross-conjugation tends to lengthen the *C*(*O*)–*N**Ar* bond and allow it to twist. In turn, the *N* can pyramidalize.

Recent calculations suggest that pyramidalization of the amide nitrogen atom is an important component of *N*–*Ar* bond rotation.²² There is evidence that various amide-type enolates are more prone to pyramidalize than their precursors, presumably because amide resonance is decreased on deprotonation.²³ We speculate that this ability to pyramidalize translates to enolates like **9** and **11** and that this is an important reason for the large decrease in the *N*–*Ar* rotation barrier.

To the extent that the N atom of the enolate can pyramidalize without a large energy penalty, the atropisomerism becomes a rotation of an sp^3-sp^2 bond rather than an sp^2-sp^2 bond. Other factors being equal, the former type of rotation is much faster.³ Compare, for example, the barriers of 12 and 13 in Figure 6.²⁴ In substrate 13, the N pyramidalizes because it is part of an amide acetal. This reduces the N–Ar rotation barrier from 29 to 23 kcal mol⁻¹.

With this detailed knowledge of the rotational preferences of *o*-methyl-substituted substrates 7 and 10, we then returned to the substrate 5 for the Hartwig cyclization. This and most other substrates used to date lack the *o*-methyl group.^{12,13} Figure 7 shows the rotational isomers of precursor 5 inside the box. Outside the box are intermediates in a catalytic cycle that was proposed by Hartwig¹² and has been widely adopted.¹³

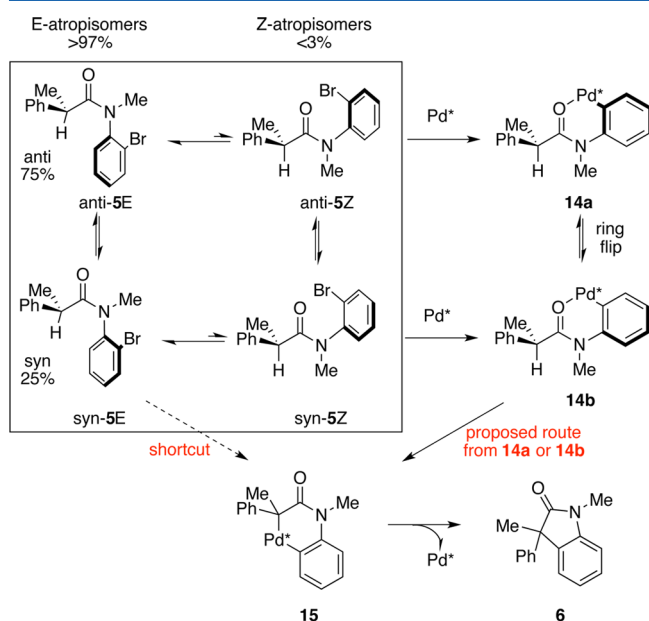


Figure 7. Steps of the Hartwig oxindole synthesis from the viewpoint of amide rotational isomers. Precursor 5 exists as eight isomers: four in the *R*-series (shown) and four in the *S*-series (not shown).

In substrate 5, the N–Ar rotation barrier is significantly decreased compared to 7/10 so the atropisomers cannot be separated.^{7a–c} Inspection of published ¹H NMR spectra of 5 and related molecules shows that there is about a 3/1 ratio of rotational isomers. These are not (*E/Z*)-amide isomers, but instead anti/syn atropisomers of the (*E*)-amide isomer (*anti*-5*E* and *syn*-5*E*). Like the *o*-methyl group in 7 (Scheme 1), the *o*-hydrogen in 5 is significantly shielded in the major antirotamer.

It is difficult to find the two minor (*Z*)-amide rotamers of 5 because the N–Ar atropisomers of 5 cannot be separated, and we could not identify clear peaks for these (*Z*)-rotamers in published spectra. So precursor 5 is at equilibrium at room temperature with an anti/syn ratio of about 75/25. Both major rotational isomers are (*E*)-amides, but there are probably trace amounts of the corresponding (*Z*)-amide rotamers.¹¹

The basic steps of the mechanism¹² are clear enough, oxidative addition, enolate formation, conversion to an Ar–Pd-enolate species, and reductive elimination, but the timing is less clear. Here we focus on conformational features and represent the chiral palladium catalysts simply as Pd*.²⁵ Hartwig proposed that the first step is oxidative addition of the

palladium species into the precursor 5 to give an intermediate 14 with the amide carbonyl group ligated to Pd*.¹² This intermediate could form directly by insertion of Pd* into a minor (*Z*)-amide rotamer, present in trace amounts.²⁶

This is a dynamic kinetic resolution because a chiral Pd-species can select between four isomeric (*Z*)-amides (*M/P*, shown; *R/S*, only *R* shown). Intermediate 14 may retain an element of axial chirality from 5, though this is now best viewed in the context of a ring conformation. In other words, if chirality is retained, then atropisomer *P*-5*Z* gives 14*a* and *M*-5*Z* gives 14*b*. If the ring flip that interconverts 14*a* and 14*b* is fast (or if the ring is planar), then the effect of the prior dynamic kinetic resolution may be erased. But if intermediates 14*a,b* are rapidly interconverting, then the next step is also a dynamic kinetic resolution.

The next key intermediate is the palladacycle 15,¹² which must result from at least two separate steps, enolate formation and amide C–N bond rotation. The deprotonation step can give (*E/Z*)-amide enolates at the enolate C=C bonds while the rotation step involves a new element of axial chirality. (The amide C–N bond can rotate two different ways during the process of complexation of Pd from O, amide bond rotation, and recompletion to C.) Reductive elimination of 15 provides the product 6.

Notice that the path from precursor to product is less direct than it could be. The amide C–N bond rotates twice, first from (*E*) to (*Z*) in the precursor 5, then later back to (*E*) in 15. Furthermore, the formation of 14 presumably occurs from the less populated (*Z*)-rotamer of 5.²⁶ A more direct process would be reaction of a syn or anti isomer of 5*E* to give 15. This shortcut could occur in as few as two steps, deprotonation and oxidative addition (in either order). So if the accepted mechanism is correct, then the steps of the longer path have the lower barriers.

Setting the possible shortcut aside and returning to the accepted mechanism, what is the stereochemistry determining step? Presumably the conversion of 15 to 6 occurs with retention of configuration at the stereocenter,^{13e} so it is not this step but a prior one. In that case, it could well involve dynamic kinetic resolution. All of the suggested intermediates have multiple isomers due to the stereocenter or enolate, the N–Ar bond or ring conformation, and of course the chiral ligand. The dynamic kinetic resolution could occur directly at the very last stage, formation of 15, or it could occur earlier, with the subsequent step(s) occurring irreversibly and with chirality transfer.

CONCLUSIONS

We have shown that *o*-haloanilide precursors of Hartwig oxindole cyclizations do not exist as planar (*Z*)-rotamers but instead twisted (*E*)-rotamers. Precursors for such cyclization typically have a stereocenter, so two diastereomeric atropisomers are present. From the standpoint of Hartwig cyclizations, the *o*-methyl group of model substrates 7 and 10 provides an artificially high barrier for atropisomerism (30–31 kcal mol⁻¹). In actual substrates like 5 lacking this Me group, the N–Ar rotation barrier is still substantial (about 15–20 kcal mol⁻¹),²¹ but atropisomerism is nonetheless rapid compared to onward reactions of these substrates under typical reaction conditions (80–100 °C). This means that the first reaction of a chiral palladium species with a precursor (amide, or its amide enolate) in the Hartwig oxindole cyclization is a dynamic kinetic resolution.

The proposed mechanism for the Hartwig cyclization¹² involves two amide C–N rotations (from (*E*) to (*Z*) and back) that are formally unnecessary. This is not to say that they cannot occur (*E/Z* rotations of the precursor are clearly rapid relative to the reaction rate). However, it is also worth considering the possibility of a more direct conversion of the major (*E*)-rotamer of the precursor **5** to the product **6** (via **15**) without any intervening amide bond rotations.

Regardless of the mechanism, all the intermediates in these cyclizations may be mixtures of multiple stereoisomers due to presence of stereocenters in the precursor and the ligand overlaid on several rotatable bonds. Accordingly, the step that determines stereochemistry in asymmetric Hartwig cyclizations could be a dynamic kinetic resolution. This might be at the penultimate step (formation of **15**), or it could occur at an earlier step with the subsequent step(s) occurring irreversibly and with chirality transfer.

The most general conclusion of this work is that axially chiral anilide enolates have a much lower barrier to atropisomerization than their amide conjugate acids. This has implications beyond Hartwig cyclizations. For example, enantiopure anilides are often obtained by resolution and re-equilibration of the undesired atropisomer,^{7–9} but the equilibration requires forcing conditions (high temperature, long times). Base-catalyzed equilibrations are an attractive alternative. And enolate reactions can be controlled either by the axial chirality of the precursors (by conducting them at low temperatures as we did with *M-10* in Scheme 3), or by dynamic kinetic resolution (by conducting them at higher temperatures). In essence, the deprotonation can be considered as a simple switch, turning on rapid rotation. Protonation turns rotation off and thereby flips the switch back.

■ EXPERIMENTAL SECTION

General Information. See the Supporting Information.

***N*-(2-Bromo-4,6-dimethylphenyl)-2-phenylpropanamide.** 2-Phenylpropanoyl chloride (279 mg, 1.65 mmol) was added to a solution of 2-bromo-3,5-dimethylaniline (300 mg, 1.5 mmol) and triethylamine (230 μ L, 1.65 mmol) in DCM (15 mL) at 0 °C under argon. The mixture was warmed to rt and monitored by TLC. After 2 h, water was added, and the phases were separated. The aqueous layer was extracted with DCM. The organic phase was washed with brine, dried over MgSO₄, filtrated, and evaporated. The residue was purified by flash chromatography (DCM) on silica gel to afford 439 mg of a white solid (88% yield): mp 128 °C; ¹H NMR (CDCl₃, 400 MHz) δ 7.45–7.37 (m, 4H), 7.33–7.31 (m, 1H), 7.19 (s, 1H), 6.93 (s, 1H), 6.73 (bs, 1H), 3.81 (q, *J* = 7.2 Hz, 1H), 2.24 (s, 3H), 2.11 (s, 3H), 1.65 (d, *J* = 7.2 Hz, 3H); ¹³C NMR (CDCl₃, 100 MHz) δ 172.5, 140.8, 138.3, 137.6, 131.1, 130.6, 130.5, 129.0, 127.9, 127.6, 121.6, 47.3, 20.6, 18.9, 18.1; FTIR (neat, cm⁻¹) 3222, 3026, 2977, 1655, 1527, 1479, 850, 718; HRMS (EI) calcd for C₁₇H₁₉BrNO 332.0650, found 332.0638.

***N*-(2-Bromo-4,6-dimethylphenyl)-*N*-methyl-2-phenylpropanamide (**7**).** To a THF slurry of NaH (40 mg, 1 mmol, 60% in oil) at 0 °C was added *N*-(2-bromo-4,6-dimethylphenyl)-2-phenylpropanamide (0.3 g, 0.9 mmol) dissolved in THF (10 mL). The reaction mixture was stirred until the solution became clear, and then iodomethane (73 μ L, 1.17 mmol) was added dropwise. The mixture was warmed to room temperature. The reaction mixture was monitored by TLC and quenched with water upon completion. The resulting mixture was extracted with EtOAc. The combined organic layers were washed with brine, dried over MgSO₄, filtrated, and evaporated. The residue was purified by flash chromatography (hex/EtOAc 95:5) on silica gel to afford 175 mg of *anti*-**7** as white solid and 95 mg of *syn*-**7** as a colorless oil (89% yield, 3:1).

Major diastereoisomer *anti*-**7**:^{13b} mp 108 °C; ¹H NMR (CDCl₃, 400 MHz) δ 7.36 (s, 1H), 7.16–7.15 (m, 3H), 6.93–6.91 (m, 2H), 6.86 (s, 1H), 3.36 (q, *J* = 6.8 Hz, 1H), 3.06 (s, 3H), 2.33 (s, 3H), 1.43 (d, *J* = 6.8 Hz, 3H), 1.41 (s, 3H); ¹³C NMR (CDCl₃, 100 MHz) δ 174.1, 141.1, 139.6, 139.1, 138.1, 131.4, 131.1, 128.3, 127.7, 126.7, 124.1, 44.0, 34.7, 20.83, 20.77, 17.4; FTIR (neat, cm⁻¹) 2985, 2934, 1659, 1477, 1451, 1375, 1280, 1117, 1090, 866, 813, 746; HRMS (EI) calcd for C₁₈H₂₁BrNO 346.0807, found 346.0798.

Minor diastereoisomer *syn*-**7**: ¹H NMR (CDCl₃, 500 MHz) δ 7.21–7.15 (m, 4H), 7.09 (s, 1H), 7.03–7.01 (m, 2H), 3.30 (q, *J* = 7.0 Hz, 1H), 3.11 (s, 3H), 2.34 (s, 3H), 2.30 (s, 3H), 1.41 (d, *J* = 7.0 Hz, 3H); ¹³C NMR (CDCl₃, 125 MHz) δ 174.0, 140.7, 139.6, 138.3, 137.6, 131.7, 130.9, 128.1, 128.0, 126.6, 124.6, 43.3, 35.7, 20.9, 20.7, 18.4; FTIR (neat, cm⁻¹) 2968, 2927, 1663, 1476, 1453, 1375, 1277, 1153, 1112, 814, 739; HRMS (EI) calcd for C₁₈H₂₁BrNO 346.0807, found 346.0798.

***N*-(2-Bromo-4,6-dimethylphenyl)-2-phenylacetamide.** Phenylacetyl chloride (160 μ L, 1.2 mmol) was added to a solution of 2-bromo-3,5-dimethylaniline (200 mg, 1 mmol) and triethylamine (420 μ L, 3 mmol) in DCM (10 mL) at 0 °C under argon. The mixture was warmed to rt and monitored by TLC. After 2 h, water was added, and the phases were separated. The aqueous layer was extracted with DCM. The organic phase was washed with brine, dried over MgSO₄, filtrated, and evaporated. The residue was purified by flash chromatography (DCM) on silica gel to afford 142 mg of a white solid (45% yield): mp 96 °C; ¹H NMR (CDCl₃, 500 MHz) δ 7.4–7.38 (m, 4H), 7.34–7.33 (m, 1H), 7.2 (s, 1H), 6.93 (s, 1H), 6.88 (s, 1H), 3.77 (s, 2H), 2.24 (s, 3H), 2.15 (s, 3H); ¹³C NMR (CDCl₃, 125 MHz) δ 169.3, 138.5, 137.6, 134.6, 131.1, 130.6, 130.5, 129.7, 129.1, 127.5, 121.7, 43.9, 20.6, 18.9; FTIR (neat, cm⁻¹) 3226, 3026, 1654, 1604, 1565, 1519, 1496, 1453, 1350, 1282, 844, 721; HRMS (EI) calcd for C₁₆H₁₇BrNO 318.0494, found 318.0468.

***N*-(2-Bromo-4,6-dimethylphenyl)-*N*-methyl-2-phenylacetamide (**10**).** To a THF slurry of NaH (186 mg, 4.7 mmol, 60% in oil) at 0 °C was added *N*-(2-bromo-4,6-dimethylphenyl)-2-phenylacetamide (1.14 g, 3.6 mmol) dissolved in THF (30 mL). The reaction mixture was stirred until the solution became clear, and then iodomethane (245 μ L, 3.9 mmol) was added dropwise. The solution was warmed to room temperature. The reaction mixture was monitored by TLC and quenched with water after 5 h. The resulting mixture was extracted with EtOAc. The combined organic layers were washed with brine and dried over MgSO₄, filtrated, and evaporated. The residue was purified by flash chromatography (Hex/EtOAc 95:5) on silica gel to afford 790 mg of a colorless oil (66% yield): ¹H NMR (CDCl₃, 600 MHz) δ 7.36 (s, 1H), 7.32–7.19 (m, 3H), 7.04–7.00 (m, 3H), 3.41 (d, *J* = 15 Hz, 1H), 3.23 (d, *J* = 15 Hz, 1H), 3.12 (s, 3H), 2.34 (s, 3H), 1.99 (s, 3H); ¹³C NMR (CDCl₃, 150 MHz) δ 171.1, 139.9, 138.4, 138.3, 134.7, 131.7, 131.2, 129.5, 128.2, 126.6, 123.9, 40.8, 34.6, 20.8, 18.1; FTIR (neat, cm⁻¹) 3028, 2922, 1665, 1476, 1433, 1369, 1305, 1152, 1103, 852, 813, 722; HRMS (EI) calcd for C₁₇H₁₉BrNO 332.0650, found 332.0629.

■ ASSOCIATED CONTENT

📄 Supporting Information

Details on resolution and equilibration studies, copies of typical chromatograms, copies of NMR spectra of all new compounds, an ORTEP diagram, and X-ray data for the crystal structure (CIF). This material is available free of charge via the Internet at <http://pubs.acs.org/>.

■ AUTHOR INFORMATION

Corresponding Author

*E-mail: daylite@pitt.edu, curran@pitt.edu.

Notes

The authors declare no competing financial interest.

ACKNOWLEDGMENTS

We thank the National Institutes of Health for funding of this work, and we thank Prof. E. Peter Kündig, University of Geneva, for samples of NHC ligands and helpful information. J.M. thanks the Fulbright Foundation for a postdoctoral fellowship award.

REFERENCES

- (1) Stewart, W. E.; Siddall, T. H. *Chem. Rev.* **1970**, *70*, 517–551.
- (2) (a) Oki, M.; Allinger, N. L.; Eliel, E.; Wilen, S. H. *Topics in Stereochemistry*; Wiley-Interscience: New York, 1983; Vol. 14, pp 1–81. (b) Gallo, R.; Roussel, C.; Berg, U. *Adv. Heterocycl. Chem.* **1988**, *43*, 174–299. (c) Eliel, E. L.; Wilen, S. *Stereochemistry of Organic Compounds*; Wiley-Interscience: New York, 1994. (d) Wolf, C. *Dynamic Stereochemistry of Organic Compounds*; RSC Publishing: Cambridge, 2008.
- (3) Examples of related cores include molecules with Nsp²-alkenyl bonds: Clark, A. J.; Curran, D. P.; Geden, J. V.; James, N.; Wilson, P. J. *Org. Chem.* **2011**, *76*, 4546–4551.
- (4) LaPlante, S. R.; D. Fader, L.; Fandrick, K. R.; Fandrick, D. R.; Huckle, O.; Kemper, R.; Miller, S. P. F.; Edwards, P. J. *J. Med. Chem.* **2011**, *54*, 7005–7022.
- (5) (a) Wilcox, C. S.; Bhayana, B. *Angew. Chem.* **2007**, *46*, 6833–6836. (b) Wilcox, C. S.; Paliwal, S.; Kim, E. *J. Am. Chem. Soc.* **1998**, *120*, 11192–11193.
- (6) Curran, D. P.; Qi, H.; Geib, S. J.; DeMello, N. C. *J. Am. Chem. Soc.* **1994**, *116*, 3131–3132.
- (7) (a) Guthrie, D. B.; Geib, S. J.; Curran, D. P. *J. Am. Chem. Soc.* **2009**, *131*, 15492–15500. (b) Petit, M.; Geib, S. J.; Curran, D. P. *Tetrahedron* **2004**, *60*, 7543–7552. (c) Curran, D. P.; Chen, C. H. T.; Geib, S. J.; Lapierre, A. J. B. *Tetrahedron* **2004**, *60*, 4413–4424. (d) Curran, D. P.; Liu, W. D.; Chen, C. H.-T. *J. Am. Chem. Soc.* **1999**, *121*, 11012–11013. (e) Ohnishi, Y.; Sakai, M.; Nakao, S.; Kitagawa, O. *Org. Lett.* **2011**, *13*, 2840–2843. (f) Kitagawa, O.; Yoshikawa, M.; Tanabe, H.; Morita, T.; Takahashi, M.; Dobashi, Y.; Taguchi, T. *J. Am. Chem. Soc.* **2006**, *128*, 12923–12931. (g) Kitagawa, O.; Takahashi, M.; Yoshikawa, M.; Taguchi, T. *J. Am. Chem. Soc.* **2005**, 3676–3677. (h) Hughes, A. D.; Price, D. A.; Simpkins, N. S. *J. Chem. Soc., Perkin Trans. 1* **1999**, 1295–1304. (i) Hughes, A. D.; Price, D. A.; Shishkin, O.; Simpkins, N. S. *Tetrahedron Lett.* **1996**, *37*, 7607–7110.
- (8) Guthrie, D. B.; Curran, D. P. *Org. Lett.* **2009**, *11*, 249–251.
- (9) Lapierre, A. J. B.; Geib, S. J.; Curran, D. P. *J. Am. Chem. Soc.* **2007**, *129*, 494–495.
- (10) (a) Dounay, A. B.; Overman, L. E. *Chem. Rev.* **2003**, *103*, 2945–2963. (b) Ashimori, A.; Bachand, B.; Calter, M. A.; Govek, S. P.; Overman, L. E.; Poon, D. J. *J. Am. Chem. Soc.* **1998**, *120*, 6488–6499. (c) Overman, L. E.; Poon, D. J. *Angew. Chem., Int. Ed. Engl.* **1997**, *36*, 518–521.
- (11) (a) Curran, D. P.; Hale, G. R.; Geib, S. J.; Balog, A.; Cass, Q. B.; Degani, A. L. G.; Hernandez, M. Z.; Freitas, L. C. G. *Tetrahedron: Asymmetry* **1997**, *8*, 3955–3975. (b) Saito, S.; Toriumi, Y.; Tomioka, N.; Itai, A. *J. Org. Chem.* **1995**, *60*, 4715–4720. (c) Itai, A.; Toriumi, Y.; Saito, S.; Kagechika, H.; Shudo, K. *J. Am. Chem. Soc.* **1992**, *114*, 10649–10650.
- (12) Lee, S.; Hartwig, J. F. *J. Org. Chem.* **2001**, *66*, 3402–3415.
- (13) (a) Liu, L.; Ishida, N.; Ashida, S.; Murakami, M. *Org. Lett.* **2011**, *13*, 1666–1669. (b) Jia, Y.-X.; Katayev, D.; Bernardinelli, G.; Seidel, T. M.; Kündig, E. P. *Chem.—Eur. J.* **2010**, *16*, 6300–6309. (c) Würtz, S.; Lohre, C.; Fröhlich, R.; Bergander, K.; Glorius, F. *J. Am. Chem. Soc.* **2009**, *131*, 8344–8345. (d) Arao, T.; Kondo, K.; Aoyama, T. *Tetrahedron Lett.* **2006**, *47*, 1417–1420. (e) Trillo, R. B.; Leven, M.; Neudörfel, J. M.; Goldfuss, B. *Adv. Synth. Catal.* **2012**, *354*, 1451–1465. (f) Pan, X. Ph.D. Thesis, University of Pittsburgh, 2012, <http://etd.library.pitt.edu/ETD/available/etd-05282011-005856/>.
- (14) More generally, palladium-catalyzed reactions between enolates and aryl halides provide diverse ring types and sizes. See, for example: (a) Honda, T.; Namiki, H.; Satoh, F. *Org. Lett.* **2001**, *3*, 631. (b) MacKay, J. A.; Bishop, R. L.; Rawal, V. H. *Org. Lett.* **2005**, *7*, 3421.
- (c) Hillgren, J. M.; Marsden, S. P. *J. Org. Chem.* **2008**, *73*, 6459. (d) Solé, D.; Serrano, O. *J. Org. Chem.* **2008**, *73*, 9372. (e) Marsden, S. P.; Watson, E. L.; Raw, S. A. *Org. Lett.* **2008**, *10*, 2905. (f) Durbin, M. J.; Willis, M. C. *Org. Lett.* **2008**, *10*, 1413. (g) Solé, D.; Serrano, O. *J. Org. Chem.* **2008**, *73*, 2476. (h) Satyanarayana, G.; Maier, M. E. *Tetrahedron* **2008**, *64*, 356. (i) Watson, E. L.; Marsden, S. P.; Raw, S. A. *Tetrahedron Lett.* **2009**, *50*, 3318. (j) Ackermann, L.; Vicente, R.; Hofmann, N. *Org. Lett.* **2009**, *11*, 4274. (k) Pan, X.; Wilcox, C. S. *J. Org. Chem.* **2010**, *75*, 6445–6451.
- (15) Control by the stereocenter is a “memory of chirality” process as defined in (a) and (b), but the term has its detractors (c). (a) Zhao, H. W.; Hsu, D. C.; Carlier, P. R. *Synthesis* **2005**, 1–16. (b) Kawabata, T.; Fuji, K. *Top. Stereochem.* **2003**, *23*, 175–205. (c) Cozzi, F.; Siegel, J. S. *Org. Biomol. Chem.* **2005**, *3*, 4296–4298.
- (16) Bruch, A.; Ambrosius, A.; Fröhlich, R.; Studer, A.; Guthrie, D. B.; Zhang, H.; Curran, D. P. *J. Am. Chem. Soc.* **2010**, *132*, 11452–11454.
- (17) Early in this work, Kündig made a racemic sample of 7 by a similar procedure and cyclized it in low ee with a chiral Pd-catalyst (ref 13b). By comparing spectra, we learned that he isolated exclusively major atropisomer. The minor atropisomer is more polar and was evidently removed during product purification. This is of little importance since the atropisomers equilibrate under the cyclization conditions.
- (18) (a) Pirkle, W. H.; Welch, C. J.; Zych, A. J. *J. Chrom. A* **1993**, *648*, 101–109. (b) Clayden, J.; Pink, J. H. *Angew. Chem., Int. Ed. Engl.* **1998**, *37*, 1937–1939.
- (19) Mekelburger, H. B.; Wilcox, C. S. In *Comprehensive Organic Synthesis*; Trost, B. M., Fleming, I., Eds.; Pergamon Press: Oxford, 1991; Vol. 2, p 99.
- (20) (a) Deetz, M. J.; Forbes, C. C.; Jonas, M.; Malerich, J. P.; Smith, B. D.; Wiest, O. *J. Org. Chem.* **2002**, *67*, 3949–3952. (b) Smith, B. D.; Goodenough-Lashua, D. M.; D’Souza, C. J. E.; Norton, K. J.; Schmidt, L. M.; Tung, J. C. *Tetrahedron Lett.* **2004**, *45*, 2747–2749.
- (21) (a) Julia, S.; Ginebreda, A.; Sala, P.; Sancho, M.; Annunziata, R.; Cozzi, F. *Org. Mag. Res.* **1983**, *21*, 573–575. (b) Adler, T.; Bonjoch, J.; Clayden, J.; Font-Bardía, M.; Pickworth, M.; Solans, X.; Solé, D.; Vallverdú, L. *Org. Biomol. Chem.* **2005**, *3*, 3173–3183. (c) For an example of pKa-dependent cross-conjugation effects on rotation barriers of heteroaryl amide C–C bonds, see: Welch, C. J.; Biba, M.; Pye, P.; Angelaud, R.; Egbertson, M. *J. Chromatogr. B* **2008**, *875*, 118–121.
- (22) Suzumura, N.; Kageyama, M.; Kamimura, D.; Inagaki, T.; Dobashi, Y.; Hasegawa, H.; Fukaya, H.; Kitagawa, O. *Tetrahedron Lett.* **2012**, *53*, 4332–4336.
- (23) Seebach, D.; Maetzke, T.; Petter, W.; Kloetzer, B.; Plattner, D. A. *J. Am. Chem. Soc.* **1991**, *113*, 1781–1786.
- (24) Ates, A.; Curran, D. P. *J. Am. Chem. Soc.* **2001**, *123*, 5130–5131.
- (25) For an expanded mechanistic discussion, see ref 13f.
- (26) Alternatively, the Pd* could oxidatively add to a major (E)-amide isomer, followed by amide bond rotation and ligation of the amide O to Pd.